Bull Math Biol (2017) 79:2773–2784
https://doi.org/10.1007/s11538-017-0348-4

Society for Mathematical Biology

ORIGINAL ARTICLE

Effects of Hydraulic Soil Properties on Vegetation Pattern Formation in Sloping Landscapes

Gerardo Severino[1] · **Francesco Giannino**[1] · **Fabrizio Cartení**[1] · **Stefano Mazzoleni**[1] · **Daniel M. Tartakovsky**[2]

Received: 13 December 2016 / Accepted: 15 September 2017 / Published online: 19 October 2017

Abstract Current models of vegetation pattern formation rely on a system of weakly nonlinear reaction–diffusion equations that are coupled by their source terms. While these equations, which are used to describe a spatiotemporal planar evolution of biomass and soil water, qualitatively capture the emergence of various types of vegetation patterns in arid environments, they are phenomenological and have a limited predictive power. We ameliorate these limitations by deriving the vertically averaged Richards' equation to describe flow (as opposed to "diffusion") of water in partially saturated soils. This establishes conditions under which this nonlinear equation reduces to its weakly nonlinear reaction–diffusion counterpart used in the previous models, thus relating their unphysical parameters (e.g., diffusion coefficient) to the measurable soil properties (e.g., hydraulic conductivity) used to parameterize the Richards equation. Our model is valid for both flat and sloping landscapes and can handle arbitrary topography and boundary conditions. The result is a model that relates the environ-

✉ Daniel M. Tartakovsky
tartakovsky@stanford.edu

Gerardo Severino
gerardo.severino@unina.it

Francesco Giannino
francesco.giannino@unina.it

Fabrizio Cartení
fabrizio.carteni@unina.it

Stefano Mazzoleni
stefano.mazzoleni@unina.it

1 Department of Agricultural Sciences, University of Naples "Federico II", via Universitá 100, Portici, 80055 Naples, Italy

2 Department of Energy Resources Engineering, Stanford University, 367 Panama Street, Stanford, CA 94305, USA

mental conditions (e.g., precipitation rate, runoff and soil properties) to formation of multiple patterns observed in nature (such as stripes, labyrinth and spots).

Keywords Vegetation pattern · Soil water flow · Sloping landscape

Mathematics Subject Classification 92D40 · 35M30 · 35C07

1 Introduction

Complex vegetation patterns (VPs) are observed in numerous regions around the world (e.g., Valentin et al. 1999; Deblauwe et al. 2008; Getzin et al. 2016). On flat grounds VPs are spots, labyrinths and gaps (von Hardenberg et al. 2001; Rietkerk et al. 2004; Gowda et al. 2014), whereas on sloping environments the typical VP is stripes (Lefever and Lejeune 1997; Klausmeier 1999; Deblauwe et al. 2008; Meron 2012). A widely accepted tenet underpinning theoretical studies of VP formation is the feedback between vegetation and water available in the soil, also known as "water redistribution hypothesis" (Sherratt and Synodinos 2012). This hypothesis states that since most of the rain falls on bare ground, which has a low infiltration rate, it runs off until it reaches vegetated areas with higher infiltration rates. This process creates a positive feedback loop between local vegetation growth and water transport toward the growth location. A typical analysis of VPs assumes that patterns start from a randomly perturbed uniform vegetation distribution and focuses on the transition between different patterns in response to the reduction in the mean (annual) rainfall (Meron 2012; Gowda et al. 2014). In this view, the terrain slope may have a fundamental impact on processes governed by water movement, due to the downhill flow both on the surface (runoff) and in the soil (Deblauwe et al. 2012; Dralle et al. 2014). A similar effect can be detected even when deterministic initial conditions mimic the effect of some localized disturbances (see, e.g., Sherratt 2016; Zelnik et al. 2016 and references therein).

Other feedback mechanisms have been hypothesized to explain VP formation in semiarid environments. Most relevant examples of such processes are local facilitation due to the reduction of evaporation by shading and the effect of the shape of the root system on the distribution of water in the soil (Meron 2016 and references therein). An additional process, which takes place on slopes, is the interception of the downhill runoff of water by vegetation. Lefever and Lejeune (1997) discussed the effects of anisotropic environmental conditions on formation of tiger bush (striped patterns). The authors showed that bands of vegetation can be either orthogonal or parallel to the anisotropy if the anisotropy enhances either negative or positive feedbacks, respectively. In the case of slopes, the anisotropy is represented by the preferential downhill flow of water both on the surface (runoff) and in the soil. This process has two main effects. First, vegetation tends to form bands and moves uphill to follow the source of water. Second, vegetation fronts deplete the resource which becomes unavailable to the plants downhill. The latter effect allows the development of another band only far enough downhill where new runoff can accumulate. Although the majority of the models rely upon the water redistribution hypothesis, it is important to understand

their physical implications, which could inadvertently lead the reader to erroneously apply the model of Klausmeier (1999) or Rietkerk et al. (2004) to unwarranted sites.

Mathematical models of VP dynamics can become very complex, since they have to account for several biophysical processes. A common approach to the problem of model selection is to adopt the principle of maximum parsimony. Thus, in line with Klausmeier (1999), we assume that the governing equation for the specific (per unit area) biomass B [ML^{-2}] is

$$\frac{\partial B}{\partial t} = D\nabla_h^2 B + cWB^2 - dB, \tag{1}$$

where the diffusion coefficient D [L^2/T] represents the plant dispersal, and $\nabla_h \equiv (\partial/\partial x_1, \partial/\partial x_2)$ denotes the two-dimensional gradient. The positive constants c [L/(MT)] and d [1/T] quantify the rate of growth and death of biomass, respectively. A survey of the values of these two parameters can be found in Marasco et al. (2014). The quantity W is typically referred to simply as "water" (e.g., Klausmeier 1999; Rietkerk et al. 2004; Cartenì et al. 2012; Marasco et al. 2014, among many others). The main assumption underlying (1) is that the biomass growth rate is proportional to plant dispersal (modeled as diffusion), water uptake and plant's natural mortality. A functional dependence $\mathcal{C} \equiv \mathcal{C}(W, B)$ of the biomass B on the soil water W can be modeled in several ways (e.g., Gierer and Meinhardt 1972; Segel and Jackson 1972). Equation (1) is based on the so-called local self-enhancement mechanism that assumes $\mathcal{C} \sim WB^2$ and covers a large class of observed cases.

We focus on the role of water distribution in determining the VP type. Rather than using a diffusion–reaction equation to describe the dynamics of the somewhat ambiguous quantity W, we use a physically based model (Richards' equation) to describe flow of water in partially saturated soils. This enables us both to express W in terms of soil water saturation and to relate soil properties and rainfall regime to the occurrence of VPs. Finally, we show how our results explain the emergence of certain patterns rather than others.

2 Model of Water Flow in Sloping Environments

A generally accepted model of fluid flow in partially saturated porous media, including water flow in soils, employs the three-dimensional Richards equation (e.g., Comegna et al. 2010, 2013; Severino et al. 2003, 2006; Fallico et al. 2016; Gómez et al. 2009 and references therein)

$$\frac{\partial \vartheta}{\partial t} = -\nabla \cdot \mathbf{q} - S, \qquad \mathbf{q} = -K_s K_r \nabla(\psi + x_3). \tag{2}$$

Here t [T] is time, $\mathbf{x} = (x_1, x_2, x_3)^\top$ [L] is the position vector with the vertical coordinate x_3 positive upward, $\vartheta(\mathbf{x}, t)$ [−] is the water content (volume of water per volume of soil), $\mathbf{q}(\mathbf{x}, t)$ [L/T] is the (Buckingham–Darcy) water flux or macroscopic (averaged) flow velocity, K_s [L/T] is the saturated hydraulic conductivity, $0 < K_r = K_r(\vartheta) < 1$ [−] is the water content-dependent relative hydraulic conductivity of the

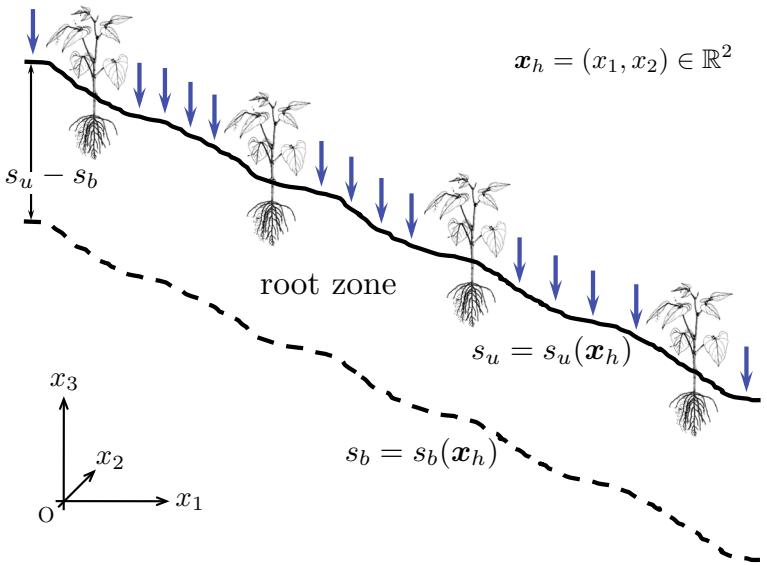

Fig. 1 Key hydrologic processes involved in vegetation pattern formation on a sloping landscape. The sloping root zone is bounded by a ground surface $s_u(x_1, x_2)$ and a surface $s_b(x_1, x_2)$ at the bottom. The infiltration flux is prescribed at the soil surface s_u. The hosting soil is horizontally unbounded (Color figure online)

soil, $\psi(\vartheta)$ [L] is the pressure head (also known as matric potential or suction) defined as the ratio $\psi \equiv p_w/\gamma_w$ between the average water pressure p_w and specific water weight γ_w. Pressure head in soils is smaller than atmospheric pressure head, i.e., $\psi < 0$. The evapotranspiration rate $S(\vartheta, B)$ [T^{-1}] depends on both water content ϑ and biomass B. It provides a field-scale representation of water uptake by roots (Hillel 1998) and can be related to a mesoscale description of water dynamics at the interface between individual roots and ambient soil (e.g., Severino and Tartakovsky 2015). Equation (2) is closed by specifying the functional forms of $K_r = K_r(\vartheta)$, $\psi = \psi(\vartheta)$ and $S(\vartheta, B)$.

We use this equation to describe water dynamics in the root zone, $s_b(\mathbf{x}_h) \le x_3 \le s_u(\mathbf{x}_h)$, where $s_u(\mathbf{x}_h)$ is the ground surface, $s_b(\mathbf{x}_h)$ is the bottom of the root zone, and $\mathbf{x}_h \equiv (x_1, x_2)^\top$ is the planar position vector (Fig. 1). Average infiltration rate p [$\mathrm{L\,T}^{-1}$] enters the model via a boundary condition

$$-\mathbf{q} \cdot \mathbf{n} = p \quad \text{for} \quad x_3 = s_u(\mathbf{x}_h) \tag{3}$$

where $\mathbf{n}$ is the unit normal vector to the surface $s_u(\mathbf{x}_h)$. The infiltration rate p is computed by subtracting runoff and other screening processes from the net precipitation rate. The bottom of the root zone, $x_3 = s_b(\mathbf{x}_h)$, is defined as soil depth at which (Bresler 1973)

$$\frac{\partial \psi}{\partial x_3} = 0 \quad \text{for} \quad x_3 = s_b(\mathbf{x}_h). \tag{4}$$

Recalling the definition of water flux $\mathbf{q}$ in (2), this boundary condition defines the bottom of a root zone as a surface below which the soil water flow is gravity-dominated. The boundary conditions (3) and (4) imply that flow in the vadose zone is largely vertical; that is the principal reason for deploying the three-dimensional Richards equation (2) rather than its one-dimensional (in the x_1 direction) counterpart used by Ursino (2005).

Ecological models deal with "water," a quantity $W(\mathbf{x}_h, t)$ whose dynamics is described in two spatial dimensions, $\mathbf{x}_h \in \mathbb{R}^2$. We define this quantity as the amount of water contained in a soil column,

$$W(\mathbf{x}_h, t) = \int_{s_b}^{s_u} \vartheta(\mathbf{x}, t) \mathrm{d}x_3, \tag{5}$$

which means that W has the units of length $[L]$. An equation for $W(\mathbf{x}, t)$ is derived by integrating (2) over x_3 (see APPENDIX for details), leading to

$$\begin{aligned} \frac{\partial W}{\partial t} &= K_s \nabla_h^2 G - K_s \nabla_h \cdot [F(s_u) \nabla_h s_u] + p\sqrt{1 + |\nabla_h s_u|^2} - K_s K_r^\star - S_t, \\ G &= \int_Z^{s_u(\mathbf{x}_h)} F \mathrm{d}x_3 \end{aligned} \tag{6}$$

where $F(\vartheta) = \int_0^\vartheta D(s)\mathrm{d}s$; $D(\vartheta)$ is the moisture diffusivity normalized by K_s [L]; $K_r^\star$ is the value of relative conductivity at $x_3 \equiv Z$; and $S_t \equiv S_t(\mathbf{x}_h, t)$ is the total rate, $[\mathrm{LT}^{-1}]$, of water consumption by plants.

We assume $K_r = \exp(\alpha\psi)$ (e.g., Tartakovsky et al. 2003) and $\vartheta = \exp(\alpha\psi)$ (e.g., Pullan 1990) where α $[\mathrm{L}^{-1}]$ is a soil parameter related to the soil's texture. The characteristic length $\lambda_c \equiv \alpha^{-1}$ is a measure of the relative importance of the capillary and gravitational forces (see White and Sully 1992; Severino et al. 2016, 2017); gravity dominates capillarity (coarse-textured soils) when $\lambda_c \to 0$ and vice versa (fine-textured soils). Then, $D(\vartheta) = 1/\alpha$, $F(\vartheta) = \vartheta/\alpha$, and (6) transforms into

$$\begin{aligned} \frac{\partial W}{\partial t} &= \frac{K_s}{\alpha}\left\{\nabla_h^2 W - \nabla_h \cdot [\vartheta(s_u)\nabla_h s_u]\right\} + p\sqrt{1 + |\nabla_h s_u|^2} - K_s K_r^\star - S_t, \\ S_t &= cWB^2 + \ell W \end{aligned} \tag{7}$$

where ℓ is the rate of the water loss in the soil by evaporation and/or drainage. This equation is exact but contains unknown $\vartheta_u \equiv \vartheta(s_u)$. While a detailed (numerical or analytical) investigation is required to compute the distribution of water content ϑ within the rooting zone (see, e.g., Severino and Tartakovsky 2015), we adopt a Dupuit-like approximation by neglecting the vertical variability of ϑ in the root zone. Then (5) gives rise to $\vartheta(s_u) \approx W/(s_u - Z) \approx aW$, where a $[\mathrm{L}^{-1}]$ is the inverse of the root zone depth (the latter approximation is not strictly necessary). Hence, (7) yields

$$\frac{\partial W}{\partial t} = \frac{K_s}{\alpha}\nabla_h^2 W - \nabla_h \cdot (\mathbf{u}_h W) + p\sqrt{1 + |\nabla_h s_u|^2} - K_s K_r^\star - S_t, \qquad \mathbf{u}_h = \frac{aK_s}{\alpha}\nabla_h s_u. \tag{8}$$

Equations (1) and (8) relate the occurrence of VPs to water distribution along the landscape. In the case of zero slope, i.e., $|\nabla_h s_u| \equiv 0$, (8) yields a generalized version of the one-dimensional model of Ursino (2005). Before proceeding further, we compare (8) with its counterpart in Sherratt (2016). The two equations are practically the same (up to a slightly different definition of the advection term). Nevertheless, there is a fundamental difference which renders our flow model more suitable for the analysis of the occurrence of VPs. Our model does not require an extra parameter (the coefficient D in Sherratt 2016) accounting for "water diffusion"; instead, it is shown to be given by the ratio, K_s/α, of well-defined (measurable) soil hydraulic properties. This allows one to relate the occurrence of VPs to: (i) soil parameters, (ii) precipitation regime and (iii) landscape's slope, thus providing a physically based explanation of the occurrence (or not) of VP in certain regions.

3 Discussion and Concluding Remarks

To elucidate the impact of soil type and slope on the emergence of VPs, we conduct numerical simulations on a square (100 m × 100 m) domain. Equations (1) and (8) are solved by a finite-difference method (for details, see Rietkerk et al. 2002). The quantities, which are allowed to vary (within a broad range), are the soil parameter α (see, e.g., Comegna et al. 2006, 2010; Severino et al. 2016) and the slope $s \equiv \nabla s_u \sim$ constant. Figure 2 depicts the spatial distribution of biomass B as predicted by our model for different $\alpha = 100, 21.5, 17.5, 10, 1\ \mathrm{m}^{-1}$ (from left to right), and slopes $s = 0, 0.3, 0.6$. The other (fixed) parameters are listed in Table 1 (Severino et al. 2003, 2010). Starting with the case of patterns in flat environments (the bottom row in Fig. 2), water is strongly retained when α is large (fine-textured soils/large capillary forces). As a consequence, almost all the infiltrated water is available for plant uptake, leading to the uniform distribution of biomass. As α decreases, the water mobility increases.

This determines a reduction of water and development of spot-type patterns. In flat landscapes, coarse-textured soils (small α) facilitate the emergence of spotted patterns, whereas fine-textured soils (large α) favor uniform vegetations. Finally, the isotropy of the biomass diffusion coefficient D implies that the shape of spots in the case of $s = 0$ is circular.

Another (and more interesting) way to look at Fig. 2 is from the bottom to the top (increasing slope) for a fixed α, i.e., for a given soil type. For fixed $K_s/\alpha \leq (8.6\,\mathrm{m\,d}^{-1})/(50\,\mathrm{m}^{-1})$, soil water retention deteriorates as the slope increases and gravity becomes dominant. As a consequence, patterns start to emerge. The effect of sloping is to produce an anisotropy in pattern formation, giving rise to an elongated "bar-type" shape (stripe) (in agreement with von Hardenberg et al. 2001; Meron et al. 2007). This is particularly pronounced at large slopes. The same transitional behavior is observed even for $K_s/\alpha \simeq (8.6\,\mathrm{m\,d}^{-1})/(10\,\mathrm{m}^{-1})$. The difference here is that the final (i.e., stripe) pattern starts from a spotted one. For $K_s/\alpha \simeq 8.6/10\,\mathrm{m}^2\,\mathrm{d}^{-1}$ the emergence of labyrinth patterns with the highest slope originates, unlike the previous case (corresponding to $\alpha \simeq 17.5\,\mathrm{m}^{-1}$), from the appearance of hexagonal-type gaps in a flat environment. Finally, for large water diffusion, e.g., for $K_s/\alpha \geq (8.6\,\mathrm{m\,d}^{-1})/(1\,\mathrm{m}^{-1})$,

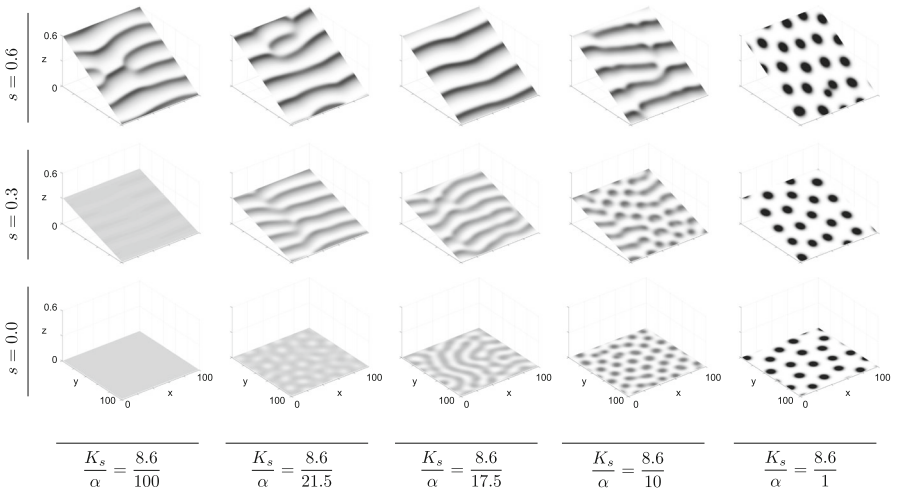

Fig. 2 Spatial vegetation patterns at $t_{\max}$ for several values of the soil diffusion coefficient K_s/α ($m^2\ d^{-1}$) with varying α (columns) and slope s (rows). The remaining parameters are listed in Table 1. Darker shades of the gray scale maps represent higher values of biomass B

Table 1 Values of the model parameters used in the numerical simulations reported in Fig. 2

Parameter	Description	Units	Value
c	Biomass's growth rate due to water uptake	$md^{-1}\,kg^{-1}$	4.5×10^{-1}
d	Death's rate of the biomass	d^{-1}	1.0×10^{-2}
p	Precipitation rate	md^{-1}	4.0×10^{-3}
D	Diffusion coefficient for biomass dispersal	m^2d^{-1}	1.0×10^{-2}
a	Inverse of the root zone width	m^{-1}	1.0
K_s	Saturated hydraulic conductivity	md^{-1}	8.6
$K_r^\star$	Relative conductivity at $x_3 \equiv Z$	–	0.0

spot-like patterns are not influenced by s because diffusion overtakes sloping. In the case of extremely sloping environments (the row corresponding to $s = 0.6$ in Fig. 2), although water is strongly retained, the slope is so steep as to prevent formation of uniform patterns (as happens for smaller s), and instead it leads immediately to stripes.

Table 2 corroborates these results by comparing the model predictions with the VPs observed in several countries for a given mean precipitation, slope and soil type. It demonstrates a good correspondence between real vegetation patterns and the ones predicted by the model simulations shown in Fig. 2.

To summarize, our study relates the analysis of Sherratt (2016) to hydraulic soil properties. By using a widely used model of flow in partially saturated porous media (Richards' equation), we recover the VPs in sloping environments predicted by Sherratt (2016). Crucially, our model provides physical insights into the effects of soil properties on VP formation:

Table 2 Review of VPmean (annual) infiltration rate p and slope, as well as by soil type (i.e., K_s/α)

Country	p (m d^{-1})	Mean slope (%)	K_s/α (m^2 d^{-1})	Pattern	References
Somalia	4.1×10^{-4}	0.60	0.10	Uniform	Hemming (1965)
Sudan	6.8×10^{-4}	0.36	1.0	Uniform	Worrall (1959)
Sudan	$(1.2 \div 1.3) \times 10^{-3}$	$0.00 \div 0.20$	1.0	Spot	Mueller et al. (2014)
Australia	$(5.2 \div 6.6) \times 10^{-4}$	$1.3 \div 1.8$	$0.10 \div 1.0$	Spot	Dunkerley and Brown (1999, 1995)
Sudan	$(1.3 \div 1.5) \times 10^{-3}$	$0.0 \div 1.2$	1.0	Spot	Mueller et al. (2014)
Mexico	7.1×10^{-4}	0.37	0.10	Stripe	Montaña et al. (1990)
Niger	1.5×10^{-3}	0.20	0.01	Stripe	Rietkerk et al. (2004)
Sudan	$(1.1 \div 1.3) \times 10^{-3}$	$0.25 \div 1.2$	1.0	Stripe	Mueller et al. (2014)

1. Coarse-textured soils do not retain water well (i.e., gravity is the dominant force), and therefore vegetational patterns are likely to be formed, in accordance with Sherratt (2016);
2. fine-textured soils strongly retain water, favoring the formation of uniform patterns.

This explains, for instance, the occurrence of VPs in arid/semiarid environments characterized by sandy (i.e., coarse) soils (see also discussions in Zelnik et al. 2015; Meron 2016). Finally, unlike the majority of the previous studies dealing with flat flow domains, we show how sloping may lead to bar-type patterns even in strongly water retaining soils wherein, in the absence of sloping, patterns are usually not observed.

In future studies, our analysis will be extended in several ways. It can be incorporated into the physics-based model of Gilad et al. (2004), which uses shallow water equations to account for overland flow (runoff) but employs a phenomenological "water diffusion" concept to deal with flow in partially saturated soils.

For the sake of simplicity, we did not consider other processes involved in the formation of VPs, such as the "litter autotoxicity" proposed by Cartenì et al. (2012) and Marasco et al. (2014), or screening effects, like interception of run-off and fog by vegetation and trees, respectively (see, e.g., Meron 2016). Future works should also investigate effects of soil properties on the cycle of water soluble toxic molecules and possible implications for the formation and stability of spatial patterns by means of a bifurcation analysis.

Acknowledgements The first author acknowledges support from "Programma di scambi internazionali per mobilitá di breve durata" (Naples University, Italy), "OECD Cooperative Research Programme: Biological Resource Management for Sustainable Agricultural Systems" (Contract No. JA00073336). D. M. Tartakovsky's research was supported, in part, by the National Science Foundation under Grant CBET-1563614.

Appendix

Integrating the Richards equation (2) over x_3 gives

$$\frac{\partial W}{\partial t} = q_3(\mathbf{x}_h, Z, t) - q_3(\mathbf{x}_h, s_u, t) - \int_Z^{s_u} (\nabla_h \cdot \mathbf{q}_h) \mathrm{d}x_3 - S_t, \tag{A1}$$

where $S_t(\mathbf{x}_h, t) \equiv \int_Z^{s_u} S(\mathbf{x}, t) \mathrm{d}x_3$ and $\mathbf{q}_h = (q_1, q_2)^\top$. According to Leibniz rule,

$$\int_Z^{s_u} (\nabla_h \cdot \mathbf{q}_h) \mathrm{d}x_3 = \int_Z^{s_u} \sum_{i=1}^{2} \frac{\partial q_i}{\partial x_i} \mathrm{d}x_3 = \sum_{i=1}^{2} \left[\frac{\partial}{\partial x_i} \int_Z^{s_u} q_i \mathrm{d}x_3 - \frac{\partial s_u}{\partial x_i} q_i(\mathbf{x}_h, s_u, t) \right]. \tag{A2}$$

Hence, (A1) yields

$$\frac{\partial W}{\partial t} = -\nabla_h \cdot \mathbf{Q}_h - q_3(\mathbf{x}_h, s_u, t) + q_3(\mathbf{x}_h, Z, t) + \mathbf{q}_h(\mathbf{x}_h, s_u, t) \cdot \nabla_h s_u - S_t, \tag{A3}$$

where $\mathbf{Q}_h = (Q_1, Q_2)^\top$ is the specific (per unit length) volumetric flow rate, [L^2/T], whose components are given by

$$Q_i(\mathbf{x}_h, t) = \int_Z^{s_u} q_i(\mathbf{x}, t)\mathrm{d}x_3, \qquad i = 1, 2. \tag{A4}$$

Next, we rewrite the equation for the soil surface as $\mathcal{F}(\mathbf{x}) \equiv x_3 - s_u(\mathbf{x}_h) = 0$. The unit normal vector to this surface is given by

$$\mathbf{n} = \frac{\nabla\mathcal{F}}{|\nabla\mathcal{F}|} = \frac{1}{|\nabla\mathcal{F}|}\left(-\frac{\partial s_u}{\partial x_1}, -\frac{\partial s_u}{\partial x_2}, 1\right)^\top. \tag{A5}$$

Hence, the boundary condition (3) takes the form

$$\mathbf{q}_h \cdot \nabla_h s_u - q_3 = p|\nabla\mathcal{F}| \quad \text{on} \quad x_3 = s_u(\mathbf{x}_h). \tag{A6}$$

The boundary condition (4), together with $q_3 = -K_s K_r \dfrac{\partial}{\partial x_3}(x_3 + \psi)$ from the second relation in (2), gives rise to the condition

$$q_3 = -K_s K_r^\star \qquad \text{on} \quad x_3 = Z, \tag{A7}$$

where $K_r^\star$ is the relative conductivity value at $x_3 = Z$. Substituting (A6) and (A7) into (A3) yields

$$\begin{aligned} \frac{\partial W}{\partial t} &= -\nabla_h \cdot \mathbf{Q}_h + p\sqrt{1 + |\nabla_h s_u|^2} - K_s K_r^\star - S_t, \\ Q_i &= \int_Z^{s_u} q_i(\mathbf{x}_h, x_3)\mathrm{d}x_3, \quad i = 1, 2 \end{aligned} \tag{A8}$$

where $S_t(\mathbf{x}_h, t)$ is the total rate of water consumption by plants, [L/T]. Substituting the definition of the Darcy flux $\mathbf{q}$ in (2) into (A4) yields

$$Q_i = -K_s \int_Z^{s_u} K_r(\vartheta)\frac{\partial\psi}{\partial x_i}\mathrm{d}x_3 = -K_s \int_Z^{s_u} D(\vartheta)\frac{\partial\vartheta}{\partial x_i}\mathrm{d}x_3, \qquad i = 1, 2 \tag{A9}$$

where $D(\vartheta)$ is the moisture diffusivity. Let $F(\vartheta) \equiv \int_0^\vartheta D(s)\,\mathrm{d}s$, then

$$Q_i = -K_s \int_Z^{s_u} \frac{\partial}{\partial x_i} F(\mathbf{x}_h, x_3)\mathrm{d}x_3, \qquad i = 1, 2. \tag{A10}$$

Using Leibniz rule,

$$Q_i/K_s = -\frac{\partial}{\partial x_i}\int_Z^{s_u} \mathrm{d}x_3\, F(\mathbf{x}_h, x_3) + F(s_u, Z)\frac{\partial s_u}{\partial x_i}, \tag{A11}$$

and substituting into (A8) leads to

$$\frac{\partial W}{\partial t} = K_s \nabla_h^2 G - K_s \nabla_h \cdot [F(s_u, Z) \nabla_h s_u] + p\sqrt{1 + |\nabla_h s_u|^2} - K_s K_r^\star - S_t. \quad \text{(A12)}$$

with

$$G = \int_Z^{s_u} F(\mathbf{x}_h, x_3) \mathrm{d}x_3. \quad \text{(A13)}$$

We assume that $K_r = \exp(\alpha\psi)$ and $\vartheta = \exp(\alpha\psi)$. Then,

$$D(\vartheta) \equiv K_r(\vartheta) \frac{\mathrm{d}\psi}{\mathrm{d}\vartheta} = \frac{1}{\alpha} \quad \text{and} \quad F(\vartheta) = \frac{\vartheta}{\alpha}. \quad \text{(A14)}$$

Hence, $G \equiv W/\alpha$, which yields (6).

References

Bresler E (1973) Simultaneous transport of solutes and water under transient unsaturated flow conditions. Water Resour Res 9(4):975–986

Cartenì F, Marasco A, Bonanomi G, Mazzoleni S, Rietkerk M, Giannino F (2012) Negative plant soil feedback explaining ring formation in clonal plants. J Theor Biol 313:153–161

Comegna A, Severino G, Sommella A (2006) Surface measurements of hydraulic properties in an irrigated soil using a disc permeameter. In: Sustainable irrigation management, technologies and policies, WIT Trans Ecol Environ (Eds: Lorenzini and Brebbia) 96, 341–353

Comegna A, Coppola A, Comegna V, Severino G, Sommella A, Vitale C (2010) State-space approach to evaluate spatial variability of field measured soil water status along a line transect in a volcanic-vesuvian soil. Hydrol Earth Syst Sci 14(12):2455–2463

Comegna A, Coppola A, Dragonetti G, Severino G, Sommella A, Basile A (2013) Dielectric properties of a tilled sandy volcanic-vesuvian soil with moderate andic features. Soil Tillage Res 133:93–100

Deblauwe V, Barbier N, Couteron P, Lejeune O, Bogaert J (2008) The global biogeography of semi-arid periodic vegetation patterns. Glob Ecol Biogeogr 17(6):715–723

Deblauwe V, Couteron P, Bogaert J, Barbier N (2012) Determinants and dynamics of banded vegetation pattern migration in arid climates. Ecol Monogr 82(1):3–21

Dralle DN, Boisramé GFS, Thompson SE (2014) Spatially variable water table recharge and the hillslope hydrologic response: analytical solutions to the linearized hillslope Boussinesq equation. Water Resour Res 50(11):8515–8530

Dunkerley DL, Brown KJ (1995) Runoff and runon areas in a patterned chenopod shrubland, arid western New South Wales, Australia: characteristics and origin. J Arid Environ 30(1):41–55

Dunkerley DL, Brown KJ (1999) Banded vegetation near Broken Hill, Australia: significance of surface roughness and soil physical properties. Catena 37(1):75–88

Fallico C, De Bartolo S, Veltri M, Severino G (2016) On the dependence of the saturated hydraulic conductivity upon the effective porosity through a power law model at different scales. Hydrol Proc 30(13):2366–2372. doi:10.1002/hyp.10798

Getzin S, Yizhaq H, Bell B, Erickson TE, Postle AC, Katra I, Tzuk O, Zelnik YR, Wiegand K, Wiegand T et al (2016) Discovery of fairy circles in Australia supports self-organization theory. Proc Natl Acad Sci USA 113(13):3551–3556

Gierer A, Meinhardt H (1972) A theory of biological pattern formation. Biol Cybern 12(1):30–39

Gilad E, von Hardenberg J, Provenzale A, Shachak M, Meron E (2004) Ecosystem engineers: from pattern formation to habitat creation. Phys Rev Lett 93(9):098105

Gómez S, Severino G, Randazzo L, Toraldo G, Otero J (2009) Identification of the hydraulic conductivity using a global optimization method. Agric Water Manag 96(3):504–510

Gowda K, Riecke H, Silber M (2014) Transitions between patterned states in vegetation models for semiarid ecosystems. Phys Rev E 89(2):022701

Hemming CF (1965) Vegetation arcs in Somaliland. J Ecol 53(1):57–67

Hillel D (1998) Environmental soil physics. Academic Press, San Diego
Klausmeier CA (1999) Regular and irregular patterns in semiarid vegetation. Science 284(5421):1826–1828
Lefever R, Lejeune O (1997) On the origin of tiger bush. Bull Math Biol 59(2):263–294
Marasco A, Iuorio A, Cartení F, Bonanomi G, Tartakovsky DM, Mazzoleni S, Giannino F (2014) Vegetation pattern formation due to interactions between water availability and toxicity in plant-soil feedback. Bull Math Biol 76(11):2866–2883
Meron E (2012) Pattern-formation approach to modelling spatially extended ecosystems. Ecol Model 234:70–82
Meron E (2016) Pattern formation-a missing link in the study of ecosystem response to environmental changes. Math Biosci 271:1–18
Meron E, Yizhaq H, Gilad E (2007) Localized structures in dryland vegetation: forms and functions. Chaos 17(3):037109
Montaña C, Lopez-Portillo J, Mauchamp A (1990) The response of two woody species to the conditions created by a shifting ecotone in an arid ecosystem. J Ecol 78(3):789–798
Mueller EN, Wainwright J, Parsons AJ, Turnbull L (2014) Patterns of land degradation in drylands. Springer, Berlin
Pullan AJ (1990) The quasilinear approximation for unsaturated porous media flow. Water Resour Res 26(6):1219–1234
Rietkerk M, Boerlijst MC, van Langevelde F, HilleRisLambers R, van de Koppel J, Kumar L, Prins HH, de Roos AM (2002) Self-organization of vegetation in arid ecosystems. Am Nat 160(4):524–530
Rietkerk M, Dekker SC, de Ruiter PC, van de Koppel J (2004) Self-organized patchiness and catastrophic shifts in ecosystems. Science 305(5692):1926–1929
Segel LA, Jackson JL (1972) Dissipative structure: an explanation and an ecological example. J Theor Biol 37(3):545–559
Severino G, Monetti VM, Santini A, Toraldo G (2006) Unsaturated transport with linear kinetic sorption under unsteady vertical flow. Transp Porous Media 63(1):147–174
Severino G, Comegna A, Coppola A, Sommella A, Santini A (2010) Stochastic analysis of a field-scale unsaturated transport experiment. Adv Water Resour 33(10):1188–1198
Severino G, Tartakovsky DM (2015) A boundary-layer solution for flow at the soil-root interface. J Math Biol 70(7):1645–1668
Severino G, Santini A, Sommella A (2003) Determining the soil hydraulic conductivity by means of a field scale internal drainage. J Hydrol 273(1):234–248
Severino G, Scarfato M, Toraldo G (2016) Mining geostatistics to quantify the spatial variability of certain soil flow properties. Procedia Comput Sci 98:419–424
Severino G, Scarfato M, Comegna A (2017) Stochastic analysis of unsaturated steady flows above the water table. Water Resour Res. doi:10.1002/2017WR020554
Sherratt JA (2016) When does colonisation of a semi-arid hillslope generate vegetation patterns? J Math Biol 73(1):199–226
Sherratt JA, Synodinos AD (2012) Vegetation patterns and desertification waves in semi-arid environments: mathematical models based on local facilitation in plants. Discret Contin Dyn Syst Ser B 17(8):2815–2827
Tartakovsky DM, Guadagnini A, Riva M (2003) Stochastic averaging of nonlinear flows in heterogeneous porous media. J Fluid Mech 492:47–62. doi:10.1017/S002211200300538X
Ursino N (2005) The influence of soil properties on the formation of unstable vegetation patterns on hillsides of semiarid catchments. Adv Water Resour 28(9):956–963
Valentin C, d'Herbès J-M, Poesen J (1999) Soil and water components of banded vegetation patterns. Catena 37(1):1–24
von Hardenberg J, Meron E, Shachak M, Zarmi Y (2001) Diversity of vegetation patterns and desertification. Phys Rev Lett 87(19):198101
White I, Sully MJ (1992) On the variability and use of the hydraulic conductivity alpha parameter in stochastic treatments of unsaturated flow. Water Resour Res 28(1):209–213
Worrall GA (1959) The Butana grass patterns. J Soil Sci 10(1):34–53
Zelnik YR, Meron E, Bel G (2015) Gradual regime shifts in fairy circles. Proc Natl Acad Sci USA 112(40):12327–12331
Zelnik YR, Meron E, Bel G (2016) Localized states qualitatively change the response of ecosystems to varying conditions and local disturbances. Ecol Complex 25:26–34